Biosensors and Bioelectronics 26 (2011) 2018–2024

Contents lists available at ScienceDirect

Biosensors and Bioelectronics

journal homepage: www.elsevier.com/locate/bios

Ultrasensitive nucleic acid biosensor based on enzyme–gold nanoparticle dual label and lateral flow strip biosensor

Yuqing He[a,b], Sanquan Zhang[a], Xibao Zhang[a,*], Meenu Baloda[b], Anant S. Gurung[b], Hui Xu[b], Xueji Zhang[c,d], Guodong Liu[b,*]

[a] Department of Dermatology, Guangzhou Institute of Dermatology, Guangzhou 510095, PR China
[b] Department of Chemistry and Biochemistry, North Dakota State University, 1301 Albrecht BLVD, Fargo, ND 58105, United States
[c] Institute of Biomedicine and Bioenergy, University of Science & Technology Beijing, No. 30 Xueyuan Rd., Beijing 100083, PR China
[d] Department of Chemistry, University of South Florida, 4202 E. Fowler Ave. CHE 205A, Tampa, FL 33620-5250, United States

ARTICLE INFO

Article history:
Received 9 June 2010
Received in revised form 27 August 2010
Accepted 31 August 2010
Available online 9 September 2010

Keywords:
Gold nanoparticles
Enzyme
DNA
Lateral flow
Biosensor

ABSTRACT

In this article, we describe an ultrasensitive nucleic acid biosensor (NAB) based on horseradish peroxidase (HRP)–gold nanoparticle (Au-NP) dual labels and lateral flow strip biosensor (LFSB). The results presented here expand on prior work (Mao et al., 2009a) by optimizing the preparation of HRP–Au-NP–DNA conjugates. It was found that sodium dodecyl sulfate (SDS) and the immobilization sequence of thiolated DNA and HRP on the Au-NP surface played very important roles to improve the sensitivity of the assay. After systematic optimization, the detection limit of current approach is 1000 times lower than that in prior work. Deposition of insoluble enzymatic catalytic product (red colored chromogen) on the captured Au-NPs at the test zone of LFSB offers a dramatic visual enhancement. Combining enzyme catalytic amplification with unique optical properties of Au-NPs, the NAB was capable of detecting of 0.01-pM target DNA without instrumentation. The NAB thus provides a rapid, sensitive, low-cost tool for the detection of nucleic acid samples. It shows great promise for in-field and point-of-care diagnosis of genetic diseases and for the detection of infectious agents.

1. Introduction

Nucleic acid biosensors (NABs) are of considerable recent interest due to their tremendous promise for obtaining sequence-specific information in a faster, simpler, and cheaper manner compared to traditional hybridization assays (Wang, 2006). Recent advances in developing such devices open up new opportunities for gene diagnostics, drug discovery, detection of infection agents, and biowarfare agents (Sassolas et al., 2008). A large number of NABs, in connection with different transducers, have been reported in the literatures (Odenthal and Gooding, 2007). However, the practical application of NABs in gene diagnosis is still in its early stage because of the high detection limit, expensive instrumentation, and complex detection procedures (Soper et al., 2006). Comparing with the low detection limit (copies of nucleic acids) of a polymerase chain reaction (PCR), the detection limit (DL) of most of NABs is relatively high and cannot meet the requirement for detecting the extremely low concentration of nucleic acids. Recently, scientists have made significant progress to improve the DL of NABs. Copies of DNA or RNA could be detected by the use of nanomaterial labels and novel signal amplification strategies (Zhang et al., 2004; Nam et al., 2004). For these highly sensitive NABs to become widely used for both clinical and research applications, reduction in the complexity of the tests (i.e., number of steps and skill base required), together with a reduction in the instrumentation and cost per test, is required. Particularly, for these NABs to be applicable at the near patient (point-of-care) or near process level, simple, easy-to-use, cost-competitive systems are required (Soper et al., 2006).

Recently, our group and others have reported lateral flow nucleic acid biosensors (LFNABs) that enable visual detection of DNA segments (Mao et al., 2009a,b; Baeumner et al., 2004). The concept was derived from a traditional immunochromotograph strip test. In this case, DNA hybridization reactions were carried out on the lateral flow device, and Au-NPs were used as labels. The captured Au-NPs on the test zone can be visualized as a red band for qualitative and quantitative detection of nucleic acid segments. Compared with other types of NABs (electrochemical, optical, and gravity), the LFNAB eliminates multiple incubation and washing steps and also minimizes the requirements for highly qualified personnel. However, the poor detection limit (nM to sub-nM) prevents its application in gene diagnosis.

Because of signal amplification, enzymes (horseradish peroxidase, alkaline phosphatase, and glucose oxidase) have been widely used as labels in the development of biosensors and bioassays (Chen et al., 2010; Patolsky et al., 2001; Hajdukiewicz et al., 2010; Wang et al., 2002). Enzymes have been also used as a label to

* Corresponding authors. Tel.: +1 701 231 8697; fax: +1 701 231 8831.
E-mail addresses: zxibao@126.com (X. Zhang), guodong.liu@ndsu.edu (G. Liu).

0956-5663/$ – see front matter © 2010 Elsevier B.V. All rights reserved.
doi:10.1016/j.bios.2010.08.079

prepare cross-flow chromatography devices for the detection of proteins (Cho et al., 2005, 2009). In these studies, the enzyme was labeled with streptavidin (or antibody) and captured on the sensor surface through DNA hybridization events (or antibody–antigen immunoreactions) and subsequent streptavidin–biotin interaction. A catalytic reaction in the presence of enzymatic substrate produced a large number of products, which would be detected with electrochemical or optical transducers. Recently, the sensitivities of assays have been enhanced by loading multiple enzymes on nano-size carriers, such as carbon nanotubes (CNT) (Wang et al., 2004) and gold nanoparticles (Au-NPs) (Li et al., 2009; Lai et al., 2009; Tang et al., 2008; Ambrosi et al., 2007). These nanocarrier-enzyme probes have significantly improved sensing performance in a variety of optical and electronic biosensing systems. In those enzyme–Au-NP-based bioassays, the localized Plasmon absorption property of Au-NP has not been utilized.

In this paper, we present an ultrasensitive LFNAB based on HRP–Au-NPs dual labels and lateral flow strip biosensor. Combining the unique optical properties of Au-NPs and enzyme catalytic amplification, which produce red colored chromogen and deposit it on the captured Au-NP and test zone of LFNAB, the LFNAB was capable of detecting of 0.01-pM target DNA without instrumentation. The promising properties of the approach are reported in the following sections.

2. Materials and methods

2.1. Apparatus

Airjet AJQ 3000 dispenser, Biojet BJQ 3000 dispenser, Clamshell Laminator, and the Guillotine cutting module CM 4000 were from Biodot Ltd. (Irvine, CA). Eppendorf Biophotometer (Eppendorf, Hauppauge, NY) was used to determine ss-DNA concentration. The portable strip reader (DT1030) was purchased from Shanghai Goldbio Tech. Co., Ltd. (Shanghai, China).

2.2. Reagents

Streptavidin, horseradish peroxidase (HRP), sucrose, sodium dodecyl sulfate (SDS), hydroxylamine, Tween 20, $HAuCl_4$, 3-amino-9-ethylcarbazole (AEC)/H_2O_2 substrate solution, 3,3′,5,5′-tetramethylbenzidine/H_2O_2 substrate solution, Triton X-100, trisodium citrate, bovine serum albumin (BSA), sodium chloride–sodium citrate (SSC) buffer 20× concentrate (pH 7.0), and phosphate buffer saline (PBS, pH 7.4, 0.01 M) were purchased from Sigma–Aldrich. Glass fibers (GFCP000800), cellulose fiber sample pads (CFSP001700), laminated cards (HF000MC100), and nitrocellulose membranes (HFB18004) were purchased from Millipore (Billerica, MA). DNA oligonucleotide probes used in this study were obtained from Integrated DNA Technologies, Inc. (Coralville, IA). The oligonucleotide sequences are as follows:

Target DNA: 5′-AGA CCA TCC TGG CTA GTC TGT TGT CTC TAC TAA AAA TA-3′;

Thiolated detection probe (used to prepare HRP–Au-NP–DNA conjugates): 5′-Thio/MC6-D/GGG GTT TCA CCG TGT TAG CCA GGA TGG TCT-3′;

Biotinylated capture probe 1 (used to prepare test line): 5′-biotin/CGC CCG GCT AAT TTT TTG TAT TTT TAG TAG AGA C-3′;

Biotinylated capture probe 2 (used to prepare control line): 5′-biotin/ATG AGA CCA TCC TGG CTA ACA CGG TGA AAC CC-3′;

2.3. Preparation of HRP–Au-NP–DNA conjugates

Au-NPs with an average diameter of 15 ± 3.5 nm were prepared according to the reported methods with slight modifications (Mao et al., 2009a). Three methods were used to prepare HRP–Au-NP–DNA conjugates.

2.3.1. Method 1

1 mL of tenfold-concentrated Au-NP solution was adjusted to pH 6.5 by adding 0.2 M NaOH; then, 25 μL of 10 mg mL^{-1} HRP were added to the above solution and the mixed solution was incubated for 2 h at 4 °C. Subsequently, the thiolated DNA (1.0 OD) was added, and the solution was kept for another 24 h at 4 °C. After incubation, 20 μL of 1% sodium dodecyl sulfate (SDS) were added to stabilize the Au-NPs with shaking at room temperature for 1 h. Finally, 75 μL of 2 M NaCl was added slowly into the solution up to a final concentration of 150 mM to "age" the DNA. The solution was kept for another 24 h at 4 °C, and the excess reagents were removed by centrifugation for 13 min at 12,000 rpm. After discarding the supernatant, the red pellets were washed twice with 0.01 M PBS (pH 7.4); centrifuged; dispersed in 1 mL of an aqueous solution containing 20 mM $Na_3PO_4{\cdot}12H_2O$, 5% BSA, 0.25% Tween, and 10% sucrose. The resulting HRP–Au-NP–DNA conjugate solution was stored at 4 °C before further use.

2.3.2. Method 2

Thiolated DNA (1.0 OD) and 25 μL of 10 mg mL^{-1} HRP were added to 1 mL of tenfold-concentrated Au-NP solution simultaneously (pH adjusted to 6.5 as stated in Method 1), and the mixture was kept for 24 h at 4 °C. Other procedures, including the addition of SDS and salts, followed those described in Method 1.

2.3.3. Method 3

Thiolated DNA probe (1.0 OD) was added to 1 mL of the tenfold-concentrated Au-NP solution. After standing at 4 °C for 24 h, the pH of the solution was adjusted at 6.5; then, 25 μL of 10 mg/mL HRP were added to the solution and the mixture was kept at 4 °C for an additional 2 h. Other procedures were the same as described in Method 1.

2.4. Sample assay procedure

The HRP–Au-NP–DNA-based LFNAB was prepared by the procedure developed by our group (Mao et al., 2009a). In a typical DNA test on the HRP–Au-NP–DNA-based LFNAB, 80 μL of sample solution containing a desired concentration of target DNA, which was prepared in a running buffer (fourfold-diluted SSC buffer containing 4% BSA) were applied to the sample application zone. After waiting for 10 min, the biosensor was washed twice by adding 20 μL of running buffer on the sample pad at 3-min intervals. Red bands were observed on the LFNAB due to the accumulation of HRP–Au-NP on the test zone and the control zone. For enzymatic amplification, 60 μL of HRP substrate solution containing 0.05% 3-amino-9-ethylcarbazole (AEC) and 0.03% H_2O_2 in 0.05 M sodium acetate buffer (pH 5.5) was added. The enzymatic reaction proceeded for 6 min to deposit red enzymatic products on the test zone and control zone of the LFNAB. The intensities of the red bands were recorded using the portable strip reader combined with the "AuBio strip reader" software. The total assay time was about 30 min.

3. Results and discussion

3.1. Principle of HRP–Au-NP dual-label-based LFNAB

HRP–Au-NP dual-label-based LFNAB combines the unique optical properties of Au-NPs with catalytic amplification of an enzyme tracer for ultrasensitive detection of nucleic acid on a lateral flow device. Our previous LFNAB (Mao et al., 2009a,b) was based on Au-NP labels, which suffered from a poor detection limit (nM or sub-nM). In the current study, we introduced an enzyme tracer,

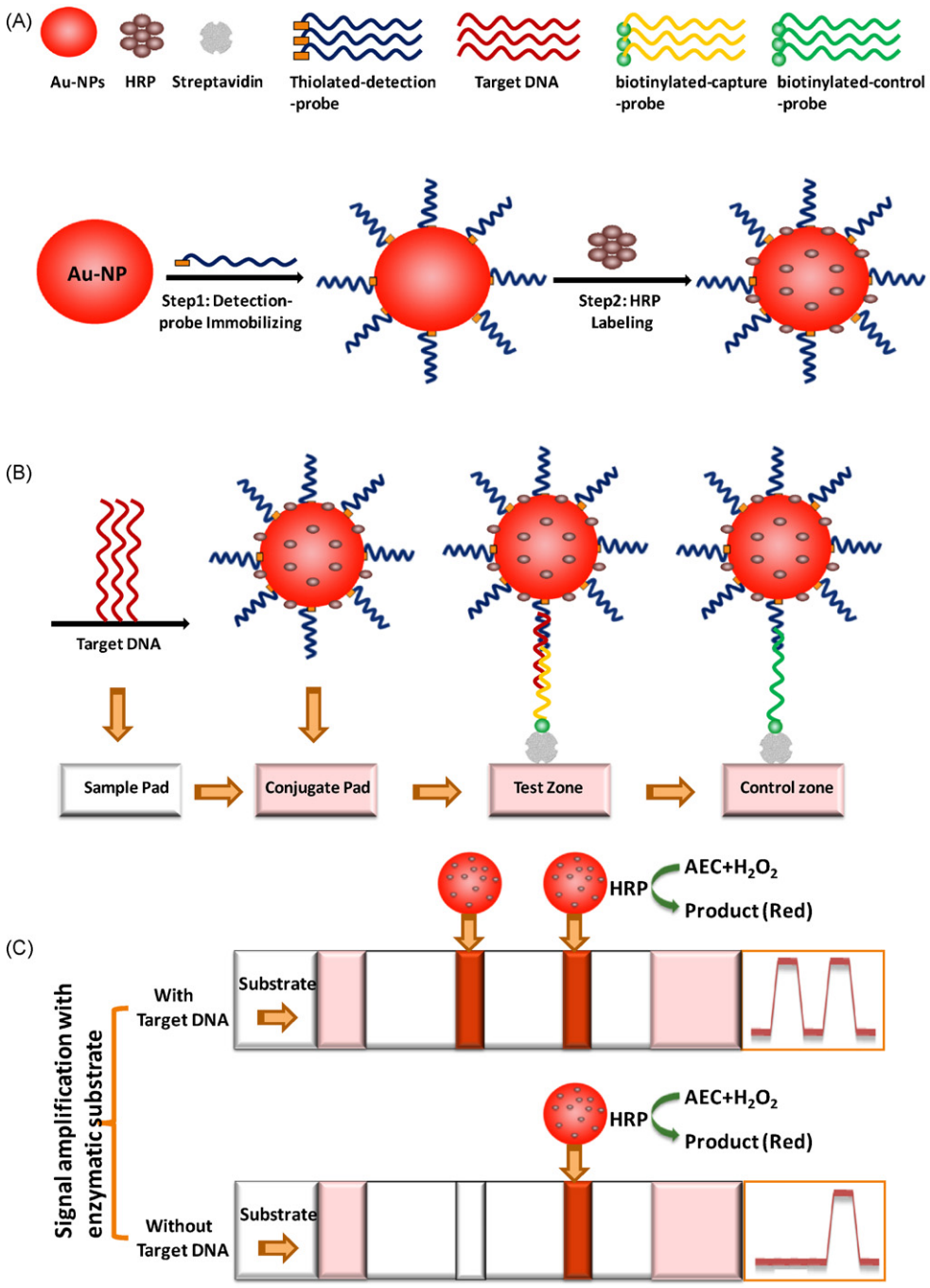

Scheme 1. (A) Schematic illustration of the preparation of HRP–Au-NP–DNA conjugates; (B) schematic illustration of capturing HRP–Au-NP–DNA conjugates on the test and control zones of lateral flow nucleic acid biosensor; (C) signal enhancement of biosensor in the presence of enzymatic substrate. AEC: 3-amino-9-ethylcarbazole.

HRP, to prepare the HRP–Au-NP dual label for LFNAB (Scheme 1A). The thiolated detection DNA probe was first introduced to Au-NP surface through self-assembling method (Scheme 1A, step 1). HRP label was then added to the mixture and adsorbed on the leftover surface of the Au-NP (Scheme 1A, step 2). The principle of HRP–Au-NP dual-label-based LFNAB is based on an on-strip sandwich DNA hybridization reaction and an enzymatic catalytic reaction; the protocol is illustrated in Scheme 1B. The HRP–Au-NP–DNA conjugates were dispensed on the conjugate pad of LFNAB; biotinylated capture DNA probe (complementary with part of target DNA) and control DNA probe (complementary with detection DNA probe on the Au-NP surface) were pre-immobilized on the nitrocellulose membrane through biotin–streptavidin interaction to form the test and control zones, respectively. The sample solution containing target DNA was applied on the sample application pad (Scheme 1B). The solution migrated by capillary action and passed the conjugate pad, and then rehydrated the HRP–Au-NP–DNA probe conjugates. The target DNA hybridized with detection DNA probe of the HRP–Au-NP–DNA conjugates to form the complex and continue to migrate along the strip. The hybrids were captured on the test zone by the second hybridization between the target DNA and the immobilized capture DNA probe. The accumulation of HRP–Au-NP in the test zone of the LFNAB was visualized as a characteristic red band. The excess of HRP–Au-NP–DNA conjugates

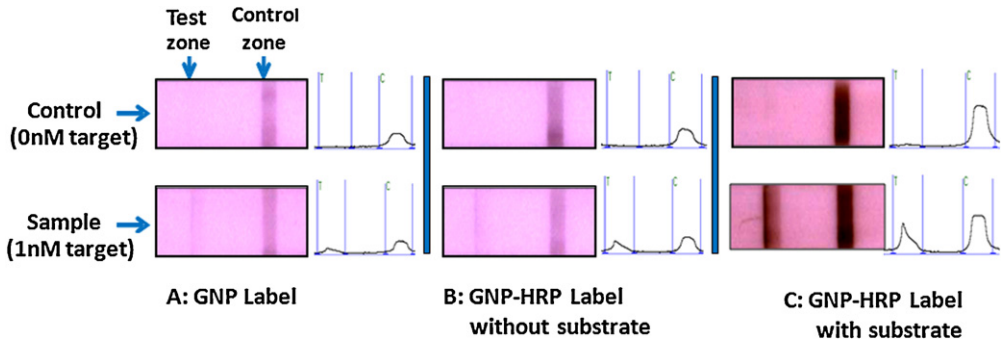

Fig. 1. Typical photo images and recorded responses of LFNABs based on Au-NP (A) and HRP–Au-NP (B and C) labels in the absence and presence of 1-nM target DNA. (A) Au-NP label based LFNAB, assay time: 24 min; (B) HRP–Au-NP dual-label-based LFNAB without applying enzymatic substrate, assay time: 24 min; (C) HRP–Au-NP dual-label-based LFNAB with enzymatic substrate. Enzymatic substrate: 0.05 M sodium acetate buffer (pH 5.5) containing 0.05% 3-amino-9-ethyl-carbazole (AEC) and 0.03% H_2O_2. Enzymatic reaction time: 6 min, the total assay time: 30 min.

continued to migrate and passed the control zone, in which the control DNA probe was immobilized. Then the excess of HRP–Au-NP–DNA conjugates were captured by the hybridization events between the detection DNA probe and the control DNA probe, thus forming a second red band. Simultaneously, numerous HRP tracers are captured on the test and control zones. Following the addition of substrate solution (AEC + H_2O_2), the enzymatic reactions produced insoluble red colored chromogen products (Graham et al., 1965), which precipitated and deposited on the test and control zones of the LFNAB. The visual effect and intensities of red bands are, thus, enhanced significantly (Scheme 1C). In the absence of target DNA, no HRP–Au-NP labels was captured on the test zone of LFNAB and no red band was observed in the test zone.

Fig. 1 presents the typical photo images and corresponding optical responses of 0-nM and 1-nM target DNA on Au-NP-based LFNAB (Fig. 1A), HRP–Au-NP-based LFNAB in the absence of enzymatic substrate (Fig. 1B), and HRP–Au-NP-based LFNAB in the presence of enzymatic substrate (Fig. 1C). Weak red bands on the test zones were observed on the Au-NP-based LFNAB and HRP–Au-NP-based LFNAB (without enzymatic substrate) in the presence of 1-nM target DNA. A bright red band was shown in the test zone of the HRP–Au-NP-based LFNAB in the presence of the substrate. The visual effect of the test line was enhanced significantly due to the precipitation and deposition of red colored chromogen products. No red band was observed on the test zone of LFNAB in the absence of target DNA (control). It is also noted that there was no background and diffusion artifacts observed on the LFNAB after the addition of the substrate. The intensities of the bands from the strip reader were shown on the right side of each image. It was found that the intensity of the test line of the HRP–Au-NP-based LFNAB increased around 8 times after the addition of substrate. Such dramatic visual enhancement offers a promising method to detect extremely low concentrations of DNA on the LFNAB.

3.2. Optimization of the immobilization procedure of HRP and DNA on the Au-NPs surface

The immobilization of HRP and thiolated DNA on Au-NPs is the most important step to prepare ultrasensitive LFNAB. The amounts of HRP and thiolated DNA on Au-NP would affect the response of LFNAB. The general approach to immobilize HRP and thiolated DNA on Au-NP is through protein adsorption (similar with the preparation of antibody–Au-NP) and self-assembling via Au–S bonds, respectively. Au-NP has been used as a carrier to load multiple HRP for sensitive DNA assays (Li et al., 2009). We compared the analytical performances of three types of HRP–Au–DNA conjugates, which were made by different immobilization procedures. In these procedures, HRP and DNA were introduced to the Au-NP solution according to different sequences. In Method 1, HRP was added into the Au-NP solution prior to the addition of the thiolated DNA. In Method 2, HRP and DNA were added into the Au-NP solution simultaneously. In Method 3, the thiolated DNA was added prior to the addition of HRP (Scheme 1A). The responses of 0.05-nM target DNA on three conjugate-based LFNABs were compared in the absence and presence of enzymatic substrate (Table 1). In the absence of substrate, there was a very weak signal (intensity 16) observed with Method 1 and no signal (intensity 0) observed with Method 2. A distinct red band (intensity 54) was observed with Method 3. It indicated that more Au-NPs were captured on Method 3 based LFNAB and that the hybridization efficiency of the conjugates prepared with Method 3 is higher than that of Methods 1 and 2. After applying the substrate solution (AEC + H_2O_2), the red bands were visible on test zones due to the deposition of red colored chromogen products. The intensity of the red band with Method 3 was 3 times more than that with Methods 1 and 2. We estimated the amounts of HRP and DNA per Au-NP by determining the HRP activities and DNA concentrations, respectively, with standard spectrophotometric assay (see details in supporting information). It seems the best immobilization efficiency was obtained with Method 2 (11 copies of HRP and 42 copies of DNA per Au-NP, Table 1), however, the best response was obtained with Method 3 (9 copies of HRP and 46 copies of DNA per Au-NP). The response difference between Methods 2 and 3 may be caused by the steric hindrance effect of HRP. More HRP on the Au-NP in Method 2 decreased the DNA hybridization efficiency and resulted in less HRP–Au-NP captured on the test zone. Therefore, Method 3 was used to prepare the HRP–Au-NP–DNA for the following experiments.

Table 1
Properties of DNA–Au-NP–HRP conjugate prepared with different methods.

	Methods		
	HRP–DNA (Method 1)	HRP + DNA (Method 2)	DNA–HRP (Method 3)
Intensities[a] of test line without substrate	16	0	54
Intensities[b] of test line with substrate	87	43	286
HRP copies per Au-NP	16	11	9
DNA copies per Au-NP	30	42	46

[a] The intensities of test line were obtained with a portable strip reader. Concentration of target DNA: 0.05 nM; assay time: 24 min.
[b] Enzymatic reaction time: 6 min.

3.3. SDS effect on the immobilization procedure of HRP and DNA on Au-NPs

It was reported that the presence of SDS aided in maximizing the DNA loading on the Au-NP because it prevented the Au-NPs from sticking either to each other or to the walls of the reaction vial (Hurst et al., 2006). In the current study, HRP was immobilized on the Au-NP surface through an adsorption process after the immobilization of DNA probes. Therefore, the addition of SDS would affect the immobilization efficiency of HRP. Two methods were used to introduce SDS: (1) SDS was added prior to the addition of HRP (DNA–SDS–HRP); (2) SDS was added after HRP addition (DNA–HRP–SDS). Fig. 2A presents the responses of the LFNABs based on the conjugates prepared with the above methods in the absence (blue bar) and presence (red bar) of the substrate. There was weak signal enhancement with the DNA–SDS–HRP method, indicating that HRP was not immobilized on the Au-NP surface effectively. The adsorbed SDS on the Au-NP occupied the thiolated DNA left vacuum, and there was not much space for the subsequent HRP adsorption. The intensities of the test line on the LFNAB increased about 3 times with the DNA–HRP–SDS method, so the addition sequence of the reagents according to DNA–HRP–SDS was used to prepare the HRP–Au-NP–DNA conjugates for the following experiments.

We studied the effect of SDS concentration during the conjugate preparation on the analytical performances of LFNABs. Fig. 2B shows the histogram for the response of 1-nM target DNA on LFNABs. The response signal (peak area) increases upon raising the SDS concentration in the conjugate solution from 0 mg mL^{-1} to 0.2 mg mL^{-1}; further increasing of the SDS concentration leads to decreases of the signal. This phenomenon can be explained by the shape of SDS aggregates on the Au-NP. At a low concentration of SDS, the SDS molecules may form hemicylindrical aggregates, whereas at high concentration, the SDS forms full cylinders (Dominguez, 2007), which may maintain the orientation of the immobilized DNA strand and improve the hybridization efficiency. Further increase of SDS concentration may cause the heavy aggregates of SDS on the Au-NP surface, leading to low hybridization efficiency. Therefore, a 0.2 mg mL^{-1} SDS was used to prepare HRP–Au–DNA conjugates for the experiments.

The amount of SDS adsorbed on the Au-NP surface is also relevant to the incubation time of SDS. The effect of SDS incubation time on the response of 1-nM target DNA on LFNABs is shown in Fig. 2C. It was found that the response of LFNAB increases with an increase of SDS incubation time up to 60 min, and then it decreases at longer incubation times. The signal loss at longer incubation times may be attributed to the formation of a large number of SDS aggregates on the Au-NP surface, which may affect the orientation of DNA probes and cause low hybridization efficiency. As a result, an incubation time of 60 min was used to prepare the conjugates for the following experiments.

After above optimizations, one can see SDS plays very important roles for the enhancement of the sensitivity of the assay. In the current study, the addition of SDS after the addition of HRP, a concentration of 0.2 mg mL^{-1} and a 60 min of incubation time would be the best conditions to prepare the HRP–Au-NP–DNA conjugates.

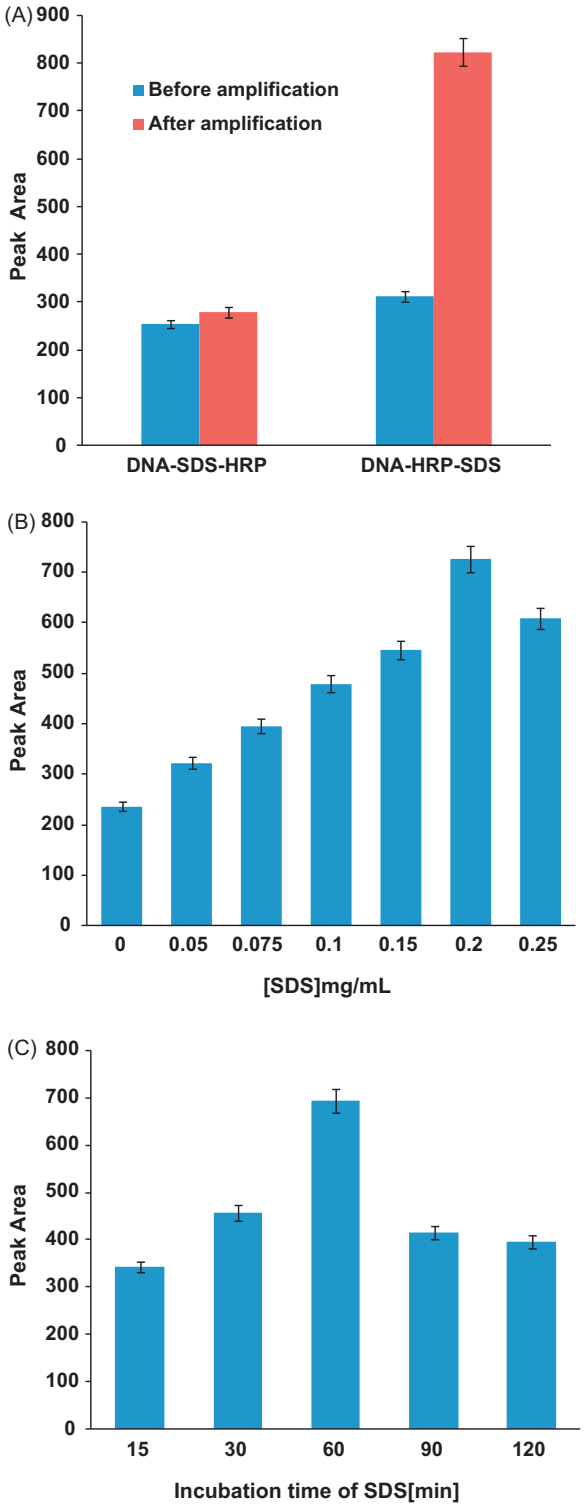

Fig. 2. Effects of SDS on the preparation of HRP–Au-NP–DNA conjugates. (A) Effect of the addition sequence of SDS on the response of LFNAB; (B) effect of SDS concentration on the response of LFNAB; (C) effect of SDS incubation time on the response of LFNAB. Target DNA concentration: 1 nM; assay time: 30 min. Other conditions are the same as in Fig. 1C. Error bars were based on three measurements ($n = 3$).

3.4. Analytical performances

After optimizing the amount of HRP–Au-NP–DNA (dispensing 2 times) and the running buffers (1/4 SSC + 4% BSA) (see details in supporting information), the HRP–Au-NP dual-label-based LFNAB was assessed for its analytical performance ability in detecting different concentrations of target DNA ranging from 0 nM to 50 nM. Fig. 3 presents the typical photo images of LFNABs in the presence of different concentrations of target DNA ranging from 0 nM to 50 nM. There is no distinct red band observed on the test zone of the LFNAB in the absence of target DNA (control), indicating negligible nonspecific adsorption under the optimized experimental conditions. The test line band is quite visible even at 0.01-pM target DNA, which can be used for the visual determination (yes/no) of target

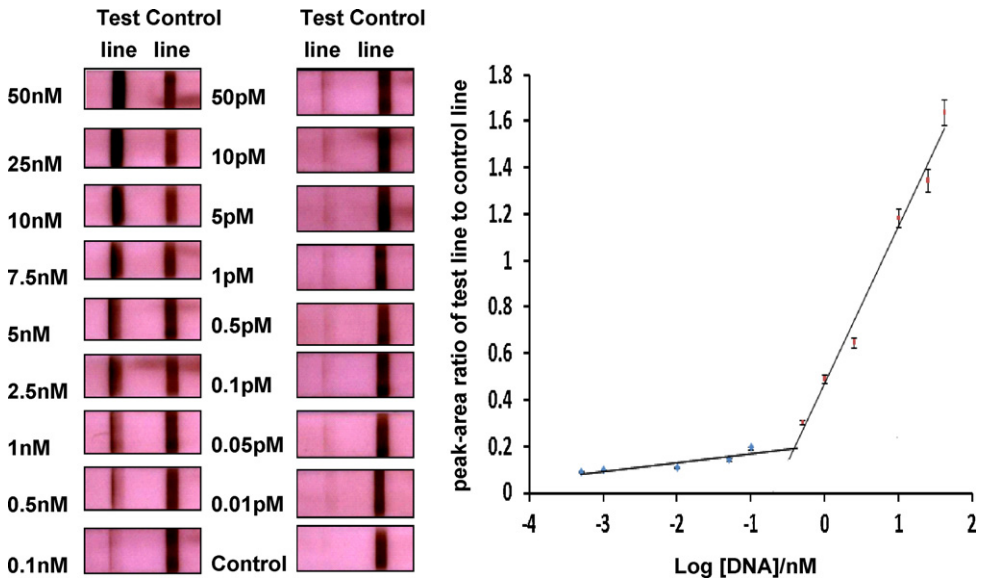

Fig. 3. Photo images (left) of the LFNABs with different concentrations of target DNA under the optimum experimental conditions and the resulting calibration curve (right). Assay time: 30 min. Running buffer: 4× SSC + 4% BSA. Dispensing cycles of the conjugates: 3. Enzymatic reaction time: 6 min. Other conditions are the same as in Fig. 1C.

DNA without instrumentation. This detection limit of visual judgment corresponded to 0.8 amol of DNA in an 80-μL sample solution, which are three orders lower than the Au-NP-based LFNAB (Mao et al., 2009a,b). It should be mentioned that the intensities of test lines are not distinguishable at the concentration range from 0.01 pM to 0.5 pM, which may be caused by the slow enzymatic catalytic reaction rate at the low concentration of enzyme and short enzymatic catalytic reaction time (6 min). Trace amount of the captured HRP would produce very small amount of enzymatic products in 6 min. The major contribution of the color of the test line would come from the captured Au-NPs, which were incapable of detecting sub-pM range of target DNA on the LFSB (Mao et al., 2009a), thus the non-distinguishable test bands.

In addition, quantitative detection was performed by recording the peak areas of the red bands in the test zone in the aid of a portable strip reader. The calibration curve (Fig. 3, right side) was prepared by plotting the peak-area ratio of test line to control line versus logarithm of the target DNA concentration. It was found that there were two linear ranges over the 0.5 pM to 50 nM range. The possible reason may come from the different contributions of red colored enzymatic products to the test line intensity at the different concentration ranges. At the 0.5 pM to 0.1 nM range, the amount of HRP captured on the test line was small. Small amount of product was produced in 6 min. So the major contributions of the test line intensity would come from the Plasmon absorption of the captured Au-NPs. At 0.1–50 nM range, large amount of product were produced, and the contribution of the enzymatic product to the test line intensity was much higher than that in the 0.5 pM to 0.1 nM range. Such different contributions from the enzymatic products resulted different sensitivities of the tests at different concentration ranges, thus two linear ranges. The quantitative detection limit of 0.3 pM, 24 amol in the 80-μL sample solution (based on S/N = 3) was estimated in connection with the 30 min assay time. This detection limit is 1000 times lower than that of the Au-NP-based LFNABs (Mao et al., 2009a,b). The LFNAB was used to detect human genomic DNA with a detection limit of 0.025 ng/mL (12.5 aM), which is much lower than that obtained with other methods (Mao et al., 2009a) (see details in supporting information).

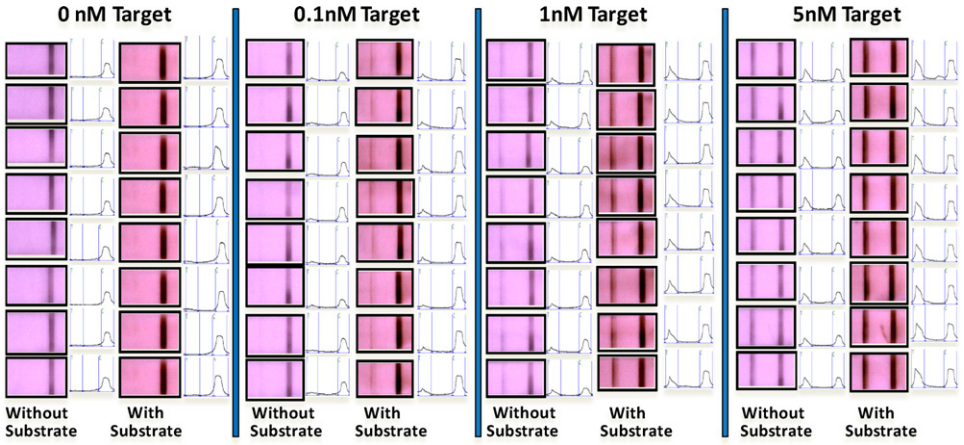

Fig. 4. Photo images and corresponding optical responses of the LFNABs in the presence of 0 nM (control), 0.1 nM, 1 nM, and 5 nM of target DNA. The photo images and optical responses were recorded on a portable strip reader prior to (left) and after (right) addition of the enzymatic substrate. Eight tests were performed with 8 different LFNABs at each concentration level. Other conditions are the same as in Fig. 3.

3.5. Reproducibility

The sensitive and specific response was coupled with high reproducibility. The reproducibility of the LFNAB was assessed by testing the sample solutions at different concentration levels. Fig. 4 presents the photo images and corresponding optical responses of 0-nM (control), 0.1-nM, 1-nM, and 5-nM target DNA before and after addition of the enzymatic substrate. Samples at the same concentration level were tested 8 times with different LFNABs from the same batch preparation. One can see that similar responses were obtained at the same concentration level. The coefficients of variation (CV) of the signals for the control, 0.1-nM, 1-nM, and 5-nM target DNA were 5.7%, 6.3%, 5.1%, and 4.6%, respectively ($n = 6$). The overall relative standard deviation was less than 7%, which indicates a good reproducibility. The reproducibility would be improved by taking the peak-area ratio of test line to control line. The CV of the signals for the control, 0.1-nM, 1-nM, and 5-nM target DNA was improved to 3.1%, 3.77%, 2.8% and 2.6%, respectively.

4. Conclusions

In conclusion, we have successfully developed an ultrasensitive nucleic acid biosensor based on HRP–Au-NP dual labels and lateral flow strip biosensor. It was found that sodium dodecyl sulfate (SDS) and the immobilization sequence of thiolated DNA and HRP on the Au-NP surface played very important roles to improve the sensitivity of the assay. Combining the unique optical properties of Au-NPs and enzyme catalytic amplification, the new lateral flow nucleic acid biosensor was capable of detecting of 0.01-pM target DNA without instrumentation. The new nucleic acid biosensor thus provides a rapid, sensitive, low-cost tool for the detection of nucleic acid samples. It shows great promise for in-field and point-of-care diagnosis of genetic diseases and for the detection of infectious agents.

Acknowledgments

This research was supported by a grant from the North Dakota Experimental Program to Stimulate Competitive Research (EPSCoR) and new faculty startup funds at North Dakota State University. Y. He acknowledges financial support from the Guangdong Provincial Natural Science Foundation of China (no. 06021655; no. 07001961; and no. 07300648), the Key Research Plan of Guangzhou Health Department, China (no. 2006-ZDi-07), and the Guangdong Province Health Department Research Fund of China (no. A2007543).

Appendix A. Supplementary data

Supplementary data associated with this article can be found, in the online version, at doi:10.1016/j.bios.2010.08.079.

References

Ambrosi, A., Castaneda, M.T., Killard, A.J., Smyth, M.R., Alegret, S., Merkoci, A., 2007. Anal. Chem. 79, 5232–5240.
Baeumner, A.J., Pretz, J., Fang, S., 2004. Anal. Chem. 76, 888–894.
Chen, X., Xie, H., Seow, Z., Gao, Z., 2010. Biosens. Bioelectron. 25 (6), 1420–1426.
Cho, J., Paek, E., Cho, I., Paek, S., 2005. Anal. Chem. 77, 4091–4097.
Cho, I., Paek, E., Kim, Y., Kim, J., Paek, S., 2009. Anal. Chim. Acta 632, 247–255.
Dominguez, H.J., 2007. Phys. Chem. B 111, 4054–4059.
Graham, R.C., Lundholm, U., Karnowsky, M.L., 1965. J. Histochem. Cytochem. 13, 150–152.
Hajdukiewicz, J., Boland, S., Kavanagh, P., Nowicka, A., Stojek, Z., Leech, D., 2010. Electroanalysis 21 (3–5), 342–350.
Hurst, S.J., Lytton-Jean, A.K.R., Mirkin, C.A., 2006. Anal. Chem. 78 (24), 8313–8318.
Lai, G., Yan, F., Ju, H., 2009. Anal. Chem. 81 (23), 9730–9736.
Li, J., Song, S., Li, D., Su, Y., Huang, Q., Zhao, Y., Fan, C., 2009. Biosens. Bioelectron. 24, 3311–3315.
Mao, X., Ma, Y., Zhang, A., Zhang, L., Zeng, L., Liu, G., 2009a. Anal. Chem. 81 (4), 1660–1668.
Mao, X., Xu, H., Zeng, Q., Zeng, L., Liu, G., 2009b. Chem. Commun., 3065–3067.
Nam, J., Stoeva, S.I., Mirkin, C.A., 2004. J. Am. Chem. Soc. 126, 5932–5933.
Odenthal, K.J., Gooding, J.J., 2007. Analyst 132, 603–610.
Patolsky, F., Lichtenstein, A., Willner, I., 2001. Nat. Biotechnol. 19, 253–257.
Sassolas, A., Leca-Bouvier, B.D., Blum, L.J., 2008. Chem. Rev. 108, 109–139.
Soper, S.A., Brown, K., Ellington, A., Frazier, B., Garcia-Manero, G., Gau, V., Gutman, S.I., Hayes, D.F., Korte, B., Landers, J.L., Larson, D., Ligler, F., Majumdar, A., Mascini, M., Nolt, D., Rosenzweig, Z., Wang, J., Wilson, D., 2006. Biosens. Bioelectron. 21, 1932–1942.
Tang, D., Yuan, R., Chai, Y., 2008. Anal. Chem. 80, 1582–1588.
Wang, J., Kawde, A., Musameh, M., Rivas, G., 2002. Analyst 127, 1279–1282.
Wang, J., Liu, G., Jan, M.R., 2004. J. Am. Chem. Soc. 126 (10), 3010–3011.
Wang, J., 2006. Biosens. Bioelectron. 21 (10), 1887–1892.
Zhang, Y., Pothukuchy, A., Shin, W., Kim, Y., Heller, A., 2004. Anal. Chem. 76, 4093–4097.